

# Translation of a leaderless reporter is robust during exponential growth and well sustained during stress conditions in *Mycobacterium tuberculosis*

A. D. Grabowska

London School of Hygiene & Tropical Medicine

N. Andreu

London School of Hygiene & Tropical Medicine

T. Cortes (✉ [teresa.cortes@lshtm.ac.uk](mailto:teresa.cortes@lshtm.ac.uk))

London School of Hygiene & Tropical Medicine

---

## Research Article

**Keywords:** Mycobacterium tuberculosis, translational regulation, mRNA transcripts

**Posted Date:** March 31st, 2021

**DOI:** <https://doi.org/10.21203/rs.3.rs-365129/v1>

**License:** © ⓘ This work is licensed under a Creative Commons Attribution 4.0 International License. [Read Full License](#)

---

## Abstract

*Mycobacterium tuberculosis* expresses a large number of leaderless mRNA transcripts; these lack the 5' leader region, which usually contains the Shine-Dalgarno sequence required for translation initiation in bacteria. In *M. tuberculosis*, transcripts encoding proteins with secondary adaptive functions are predominantly leaderless and the overall ratio of leaderless to Shine-Dalgarno transcripts significantly increases during growth arrest, suggesting that leaderless translation might be important during persistence in the host. However, whether these two types of transcripts are translated with differing efficiencies during stress conditions that induce growth arrest and during optimal growth conditions, is unclear. Here, using bioluminescent reporter strains, we detect robust leaderless translation during exponential *in vitro* growth and we show that leaderless translation is more stable than Shine-Dalgarno translation during adaptation to stress conditions. Upon entrance into nutrient starvation and after nitric oxide exposure, leaderless translation is significantly less affected by the stress than Shine-Dalgarno translation. Similarly, during the early stages of infection of macrophages, the levels of leaderless translation are more stable than those of Shine-Dalgarno translation. These results suggest that leaderless translation may offer an advantage in the physiology of *M. tuberculosis*. Identification of the molecular mechanisms underlying this translational regulation may provide insights into persistent infection.

## Introduction

Tuberculosis, caused by *Mycobacterium tuberculosis*, is mainly a pulmonary disease and the leading cause of death worldwide from a single infectious agent, with nearly 1.5 million deaths each year<sup>1</sup>. In 2018, world tuberculosis incidence exceeded 10 million people<sup>1</sup>, and it is estimated that a quarter of the human population (1.7 billion individuals) is latently infected with *M. tuberculosis*<sup>2</sup>. This reflects the complex life cycle of this pathogen, that can involve prolonged periods of asymptomatic infection, where the bacteria enter a non-replicating state, prior to the onset of disease. During this process, bacteria have to adapt to diverse stresses, including nutrient and oxygen limitation, and exposure to reactive oxygen and nitrogen species within host cells<sup>3</sup>, primarily alveolar macrophages.

The downregulation of key life processes, like transcription and translation, has been associated with *M. tuberculosis* tolerance to stresses, usually via non-replicating persistence<sup>4,5</sup>. Biological adaptation mediated by translation regulation has been increasingly associated to changes in ribosomal composition, both in bacteria and eukaryotes<sup>6,7</sup>. These changes in ribosomal composition would result in the selective translation of different types of mRNA transcripts. In bacteria, the canonical transcript structure includes a 5' untranslated region (5' UTR) that harbours important regulatory sequences like the Shine-Dalgarno sequence required for translation initiation. Canonical translation of bacterial transcripts is initiated by binding of the Shine-Dalgarno sequence to the complementary region of 16S ribosomal RNA in the 30S small subunit of the ribosome<sup>8</sup>. But bacterial transcripts that completely lack a 5'UTR and hence the Shine-Dalgarno sequence, known as leaderless transcripts, also exist<sup>9,10</sup>. The absence of a Shine-Dalgarno sequence has important implications for the initiation of translation. In *Escherichia coli*, leaderless transcripts are translated with low efficiency when a 70S ribosome directly binds to the ATG start codon<sup>11,12</sup>. This preference can be altered by antibiotics or toxin-antitoxin systems, that generate subpopulations of specialised ribosomes that selectively translate leaderless transcripts<sup>13,14</sup>. Previous research in *M. tuberculosis* has shown that approximately 25% of its genes are expressed as leaderless transcripts<sup>15,16</sup>, a substantially higher percentage than that reported in other bacterial pathogens (1.2-3%)<sup>17-20</sup>. In the model organism *Mycobacterium smegmatis*, which also contains a similar percentage of leaderless transcripts to that of *M. tuberculosis*, comparable translation rates for canonical and leaderless transcripts have been reported<sup>16,21</sup>. Altogether, this suggests that leaderless translation might have a more central role in the regulation of mycobacterial physiology than in that of *E. coli*. Indeed, proteins with secondary adaptive functions, like toxin-antitoxin systems, are generally leaderless in *M. tuberculosis* and the overall ratio of leaderless to canonical Shine-Dalgarno transcripts increases during incubation in a starvation model of growth arrest<sup>15</sup>. These observations suggest that Shine-Dalgarno and leaderless transcripts might be differentially translated during different stresses, such as during nutrient deprivation and macrophage infection; however, this has not been investigated.

Here we aimed to better understand the role of leaderless translation in the response of *M. tuberculosis* to stress and during infection. To this end, we quantified translation differences between leaderless and Shine-Dalgarno transcripts during different growth conditions and during macrophage infection using leaderless and Shine-Dalgarno luminescent *M. tuberculosis* reporter strains. Quantification of luminescence levels during exponential growth and during exposure to nitric oxide (NO), nutrient starvation and infection of macrophages revealed robust and sustained leaderless translation in *M. tuberculosis*. Our results suggest that leaderless translation may offer an advantage to Shine-Dalgarno translation during adaptation to different growth conditions.

## Results

### ***Construction of Shine-Dalgarno and leaderless M. tuberculosis reporter strains***

To study the role of leaderless translation in *M. tuberculosis* response to stress and infection, we first devised a system to easily quantify translation in *M. tuberculosis* by engineering a promoterless firefly luciferase (FFluc) encoding vector that could be used to generate suitable integrative translational reporters. As backbone we used the mycobacterial integrating vector pMV306<sup>22</sup> with five copies of the transcriptional terminator *trp*<sup>23</sup>. We then cloned the *ffluc* coding region codon-optimized for *M. tuberculosis* from pMV306hsp+FFluc<sup>24</sup> and removed the optimised Shine-Dalgarno sequence to create pTC1 (Supplementary figure 1A). Bioluminescence production in the resulting strain was not significantly different to that in the

H37Rv wild-type strain with no *ffluc* gene, indicating that there was no background transcription and translation of the *ffluc* gene in the promoterless vector (Supplementary Figure 1B).

To compare translational efficiency between leaderless and Shine-Dalgarno transcripts, we selected the *desA1* (Rv0824c) and *desA2* (Rv1094) gene pair which encode homologous acyl-ACP desaturases sharing 30% primary sequence identity. Both genes are strongly expressed during exponential growth and have a typical TANNNT -10 promoter motif; however, while *desA1* contains a 5'UTR with the Shine-Dalgarno sequence, *desA2* is expressed as a leaderless transcript<sup>15</sup>. We obtained the Shine-Dalgarno reporter construct pTC2 by fusing the *desA1* 50 bp promoter region, the 5'UTR and the region encoding the first six amino acids of *desA1* to *ffluc* in pTC1 (Figure 1A); similarly, we generated the leaderless reporter construct pTC3 by fusing the *desA2* 50 bp promoter region and the region encoding the first six amino acids of *desA2* to *ffluc* in pTC1 (Figure 1A). To make sure that any differences observed between the Shine-Dalgarno and leaderless reporters were due to translational regulation and not to transcriptional regulation, we swapped the 50-bp *desA1* and *desA2* promoters in pTC2 and pTC3 to create the Shine-Dalgarno reporter pTC4 and the leaderless reporter pTC5, respectively (Figure 1A). All reporter sequences were verified by sequencing and plasmids were subsequently electroporated in *M. tuberculosis*. Successful integration was verified by polymerase chain reaction (PCR) followed by sequencing. Additionally, we verified that transcription of the reporters was driven by the desired promoter by determining the transcriptional start sites using 5' rapid amplification of cDNA ends (RACE). Finally, we verified translation of the *FFluc* reporter by measuring luminescence of the reporter strains over a 5-day period of exponential growth as an indirect measurement of protein expression. All reporter strains showed comparable levels of luminescence suggesting they have comparable levels of luciferase production (Figure 1B). As a result, we selected the Shine-Dalgarno pTC2 and leaderless pTC5 reporter pair, for which pTC2 contains a naturally occurring canonical Shine-Dalgarno organisation for further experiments.

### ***The leaderless reporter is robustly translated in M. tuberculosis during exponential and stationary in vitro growth***

Our results so far suggested that the leaderless reporter was translated with similar efficiency to that of the Shine-Dalgarno reporter at least during exponential growth (Figure 1B). To identify possible differences in the translation efficiencies of the Shine-Dalgarno and leaderless reporters that could be associated with the growth status of the bacteria we used pTC2 and pTC5 to closely monitor luminescence production during the switch from exponential to stationary growth. As a control, we also measured translation of the reporters in *M. smegmatis* as experiments using fluorescent reporters have shown that leaderless translation in *M. smegmatis*, a close relative of *M. tuberculosis* that also encodes a high percentage of leaderless proteins in its genome<sup>15,16</sup>, has similar efficiency to that of a Shine-Dalgarno reporter<sup>21</sup>. Additionally, we measured translation of the reporters in *E. coli*, a bacterium with scarce leaderless transcripts that are translated at low levels by the 70S monosome<sup>25</sup>.

Introduction of the reporter vectors did not affect bacterial growth in any of the three bacterial models tested (Figure 2A-C). As predicted, during exponential growth luminescence production from the leaderless reporter in *E. coli* was 1 log lower than that from the Shine-Dalgarno reporter (one-way ANOVA,  $p < 0.0001$ ; Figure 2D and 2G). By contrast, in *M. smegmatis* luminescence from the leaderless reporter was significantly higher than that from the Shine-Dalgarno reporter (one-way ANOVA,  $p < 0.001$ ) (Figure 2E and 2H), whereas in *M. tuberculosis* luminescence production of the leaderless reporter was comparable to that of the Shine-Dalgarno reporter (Figure 2F and 2I). Upon entrance into stationary growth, median luminescence levels increased for both reporters in *E. coli*, but the increase was not statistically significant in the case of the leaderless reporter (Figure 2G). In *M. smegmatis*, the translation of the Shine-Dalgarno reporter significantly decreased whilst the median levels of leaderless translation were maintained (one-way ANOVA,  $p < 0.0001$ ) (Figure 2H). In the case of *M. tuberculosis*, Shine-Dalgarno translation was not significantly reduced upon entrance into stationary growth, while leaderless translation was significantly increased (one-way ANOVA  $p < 0.0001$ ) (Figure 2I).

In summary, our results show a robust translation of the leaderless reporter during exponential growth in *M. tuberculosis*, to a level comparable to that of the Shine-Dalgarno reporter, and a significant increase in leaderless translation upon entrance into stationary growth.

### ***The preference for translation of the leaderless reporter varies during different in vitro stresses in M. tuberculosis***

Our results indicated that the ratio of translation of leaderless and Shine-Dalgarno transcripts differed during exponential and stationary phase in *M. tuberculosis*. Next, we studied whether this was also the case during stress conditions. In particular, we determined the translation of leaderless and Shine-Dalgarno reporters in *M. tuberculosis* during nutrient starvation and following a transient stress with a sub-lethal concentration of NO. These two conditions are representative of conditions encountered by *M. tuberculosis* during non-replicating growth<sup>26</sup> and active infection in humans<sup>27,28</sup>, respectively. In each condition tested, we addressed translation kinetics of the leaderless and Shine-Dalgarno reporters by measuring luminescence produced from the pTC2 and TC5 reporter vectors and quantified changes at the transcriptional level through quantitative real-time PCR to rule out changes due to differences in promoter activities.

For the nutrient starvation experiments, cells growing exponentially in nutrient-rich media were washed with PBS and used to inoculate (time 0). PBS (nutrient starvation) and nutrient-rich media (7H9 media, control) cultures were incubated for 28 days. The control cultures grew exponentially for 5 days before reaching stationary phase (Figure 3A). These cultures reached stationary phase 2 days earlier than the cultures in Figure 2C, likely because of the higher starting OD (see Material and methods). As expected, nutrient limitation affected the growth and translation efficiency of both the leaderless and Shine-Dalgarno *M. tuberculosis* reporter strains compared to those in the control cultures (Figures 3A and 3B). In both the control and the nutrient starvation cultures, the leaderless reporter was translated at a higher level than the Shine-Dalgarno reporter (multiple t-tests,  $p < 0.03$ ) (Figure 3B). When comparing changes in the translation of the reporters during nutrient starvation compared to that during control conditions, we

found a significant decrease in the translation of the Shine-Dalgarno reporter compared to that of the leaderless reporter after 24 hours of nutrient starvation (multiple t-tests,  $p < 0.001$ ) (Figure 3C). This difference was not driven by transcriptional changes, as transcription levels of the Shine-Dalgarno and leaderless reporters did not change significantly (Tukey's multiple comparisons test,  $p > 0.163$ ) (Figure 3D). This more pronounced effect of the stress on Shine-Dalgarno-mediated translation was transient, as we observed comparable reduction of translation of both types of reporters at later timepoints (Figure 3C).

Next, we studied changes in translation during exposure to a sub-lethal concentration of NO by monitoring changes in luminescence in exponentially growing cultures of the *M. tuberculosis* leaderless and Shine-Dalgarno reporter strains exposed to 0.25 mM NO or sodium hydroxide (used to dissolve the NO adduct, see Material and methods) for 7 days. As expected, exposure to NO caused a rapid but transient growth arrest of both the Shine-Dalgarno and leaderless reporter strains that could be observed already at 24 hours post-NO exposure (Figure 4A). Throughout the experiment, the leaderless reporter was translated at a higher level than the Shine-Dalgarno reporter in both the stressed and the control cultures (multiple t-tests,  $p < 0.03$ ) (Figure 4B). Indeed, although the transient inhibition in growth resulted in a decrease in translation of both reporters compared with the corresponding controls, both reporters were affected to a similar degree and hence translation of the leaderless reporter was higher than that of the Shine-Dalgarno reporter (Figures 4B and 4C). Forty-eight hours after NO treatment started, both reporter strains resumed growth and luminescence suggesting that they had recovered from the stress (Figures 4A and 4B). At this point, the percentage of translation of the leaderless reporter in comparison with that in the corresponding control was significantly higher than that of the Shine-Dalgarno reporter (27% vs 14%, respectively, multiple t-tests,  $p < 0.002$ ), suggesting a quicker recovery of leaderless translation following exposure to NO stress (Figure 4C). These differences were not driven by transcriptional changes, as we found no significant differences in the transcription levels of Shine-Dalgarno and leaderless transcripts (Tukey's multiple comparisons test,  $p > 0.162$ ) (Figure 4D).

Overall, the results show that leaderless translation is significantly less affected by nutrient starvation and recovers more quickly from nitrosative stress than Shine-Dalgarno translation.

#### ***Translation of the leaderless reporter is less affected during the early stages of macrophage infection***

Finally, we studied translation efficiency of Shine-Dalgarno and leaderless transcripts during *M. tuberculosis* intracellular growth in macrophages. To this end we measured luminescence of the reporter strains during infection of PMA-activated THP-1 cells. We used an MOI of 10 to ensure enough luminescence from the reporters was detected.

Following infection of THP-1 cells, no increase in luminescence and growth was observed for the reporter strains during the first 24 hours (Figure 5A and 5B). At 48 hours post infection, both reporter strains resumed growth and translation, suggesting that they had adapted to the intracellular environment. Luminescence from the leaderless reporter was higher than that from the Shine-Dalgarno reporter and this difference was significant between 24 and 72 hours post infection (multiple t-tests,  $p < 0.002$ ) (Figure 5B). To quantify how translation of the leaderless and Shine-Dalgarno reporters responded during the different stages of macrophage infection, we normalised the luminescence levels of the reporters at different time points against the luminescence levels at time 0. This revealed that during the first 48 hours of infection, before bacterial growth resumed, translation of the leaderless reporter was less affected than that of the Shine-Dalgarno reporter, and this difference was statistically significant at 48 hours post infection (multiple t-test,  $p < 0.05$ ) (Figure 5C). As growth resumed following adaptation to the intracellular environment, the translation efficiency of both types of transcripts increased to comparable levels (Figure 5C). Our data show that during the early stages of macrophage infection, the translation efficiency of the leaderless reporter is significantly less affected by exposure to the intracellular host environment than that of the Shine-Dalgarno.

## **Discussion**

Adaptation of *M. tuberculosis* to stress conditions by regulation of gene and protein expression is key for survival of this pathogen in the hostile intracellular environment. In this study we aimed to better understand the role of leaderless translation in the response of *M. tuberculosis* to stress and during infection. Our results indicate that the leaderless reporter is translated more efficiently during adaptation to stress conditions in *M. tuberculosis*. Luminescence production of the leaderless reporter was less affected than that of the Shine-Dalgarno reporter upon entrance into nutrient starvation and during the recovery phase from nitrosative stress, as well as during the early stages of macrophage infection.

Transcription of leaderless transcripts significantly increases during nutrient starvation-induced growth arrest in *M. tuberculosis*<sup>15</sup> and in other bacteria, like *E. coli*, leaderless transcripts can be preferentially translated during unfavourable conditions like those triggered by exposure to antibiotics or toxin-antitoxin systems<sup>13,14</sup>, suggesting that these transcripts can play an important role in the bacterial adaptation to stress conditions. We selected nutrient starvation, exposure to nitric oxide and infection of macrophages to further study their effect on the translation levels of our leaderless and Shine-Dalgarno reporters. Although ribosome profiling analysis has not revealed an overall difference in the translation efficiency of leaderless transcripts compared to that of Shine-Dalgarno transcripts<sup>29</sup>, our results show that translation of the leaderless reporter, measured as luminescence production, is less affected than that of its matched Shine-Dalgarno reporter. However, this effect is mostly transient, as shown by leaderless and Shine-Dalgarno reporters reaching comparable levels of luminescence after the initial phases of nutrient starvation-induced growth arrest and growth in THP-1 cells. These results suggest that leaderless translation could offer an advantage to Shine-Dalgarno translation under some growth conditions, including starvation-induced growth arrest, even if it just means a faster adaptation to environmental changes.

Translation of the leaderless reporter was robust in our system, confirming what has been shown at genome-wide level in both *M. smegmatis* and *M. tuberculosis*<sup>16,29</sup>, and highlighting an important difference with the *E. coli* model, where leaderless translation is performed with low efficiency by the *E. coli* ribosome<sup>25,30,31</sup>. In fact, introduction of our leaderless reporter into *E. coli* cells showed a 1 log reduction in luminescence levels compared to that of the Shine-Dalgarno reporter, highlighting mechanistic differences between the two bacterial models. The recently solved crystal structures of the *M. tuberculosis* and *M. smegmatis* ribosomes have revealed two novel ribosomal proteins and a significant degree of structural heterogeneity<sup>32,33</sup>, suggesting that either mycobacterial ribosomes have a greater capacity to efficiently translate different transcript organisations or the existence of subpopulations of ribosomes with the ability to preferentially translate different transcripts. In this respect, the identification of at least four additional ribosomal proteins, which can be alternatively incorporated into the ribosome in response to zinc starvation in *M. smegmatis*<sup>34–36</sup>, and the identification of ribosome-associated proteins under non-optimal growth conditions in both *M. smegmatis* and *M. tuberculosis*<sup>37,38</sup>, contribute to the body of recent literature highlighting further layers of translational regulation in this pathogen. Our results here reported, where we have detected widespread translation of the leaderless and Shine-Dalgarno reporters under different growth conditions in *M. tuberculosis*, will support the hypothesis that *M. tuberculosis* ribosomes have the capacity to efficiently translate different transcript organisations rather than relying on a translational reprogramming for selective translation of different transcripts.

We have observed no differences in luminescence production for the leaderless and Shine-Dalgarno reporters during exponential growth in *M. tuberculosis*. A recent study has investigated the impact of leadered and leaderless translation in *M. smegmatis* during exponential growth using fluorescent translational reporters<sup>21</sup>. Briefly, the 5'UTR sequence of sigma factor sigA was used as a representative of leadered translation for the construction of the fluorescent reporters, and compared its fluorescence to that of a leaderless reporter (devoid of the 5'UTR sequence) as well as another leadered reporter carrying the 5'UTR from the semi-synthetic promoter p<sub>myc1</sub>tetO instead of the sigA 5'UTR. They found that the leaderless reporter was significantly less fluorescent than the leadered counterpart carrying the semi-synthetic 5'UTR, suggesting that leaderless transcripts may be translated with less efficiency; but when leaderless fluorescence was compared to that of the reporter carrying the native sigA 5'UTR structure, they observed no significant differences in fluorescence levels<sup>21</sup>, similarly to what we report in this study with luminescent reporters. Interestingly, these findings highlight how different 5'UTR conformations, including those without a Shine-Dalgarno sequence, can severely impact translation rates in mycobacteria and needs to be taken into consideration when drawing more general conclusions about gene regulation in *M. tuberculosis*.

We selected the desA1 and desA2 gene pair as representatives of the Shine-Dalgarno and leaderless transcripts in *M. tuberculosis* on the basis of their protein shared homology, widespread expression<sup>15</sup> and conserved features within their promoters, like the presence of a -10 TANNNT sigA consensus motif<sup>39</sup> or the use of ATG as a start codon<sup>15,40</sup>. We used luminescent reporters as they provide a sensitive and convenient measurement of protein expression in bulk *M. tuberculosis* cultures<sup>24</sup>. As we have only used one pair of leaderless and Shine-Dalgarno reporters to quantify differences in luminescence production, future work is needed to correlate if the changes here reported are representative of the leaderless transcripts as a whole and to mechanistically identify differences in their translation to that of Shine-Dalgarno transcripts in *M. tuberculosis*.

This work represents the first report where individual luminescent reporter strains have been used to describe differences in the translation of mRNA transcripts with different architectures during different growth conditions in *M. tuberculosis*. Our results show that during the early stages of starvation-induced growth arrest, exposure to NO and growth in THP-1 cells, leaderless translation is transiently less affected than that of Shine-Dalgarno translation. Altogether, our data suggest that differential translation of different types of transcripts, and in particular the translation of transcripts lacking a leader sequence, may have particular importance in the physiology of *M. tuberculosis*.

## Materials And Methods

### Bacterial strains and growth conditions

*Mycobacterium tuberculosis* H37Rv (SysteMTb), *Mycobacterium smegmatis* mc<sup>2</sup>155<sup>41</sup> and *Escherichia coli* NEB-5a and NEB-10β (New England Biolabs UK Ltd) were used in this study. All the strains were grown at 37°C. All work involving live *M. tuberculosis* was performed in a dedicated Biosafety Level 3 (BSL 3) laboratory. *M. tuberculosis* and *M. smegmatis* were grown on Middlebrook 7H11 agar medium (BD Diagnostics) supplemented with 0.5% glycerol and 10% oleic acid albumin-dextrose-catalase (OADC) enrichment (BD Diagnostics). Liquid cultures of mycobacteria were grown in Middlebrook 7H9 broth (BD Diagnostics) supplemented with 0.2% glycerol, 10% albumin-dextrose-catalase (ADC) enrichment (BD Diagnostics) and 0.05% Tween 80 (Sigma). For the nutrient starvation and nitric oxide expression screens, *M. tuberculosis* was cultured in 100 ml of liquid medium in 1L roller bottles rolling at 2 rpm, unless stated otherwise. *E. coli* was cultured on Luria-Bertani (LB) agar and in LB liquid medium. Kanamycin was added where appropriate [25 µg ml<sup>-1</sup> for mycobacteria, 50 µg ml<sup>-1</sup> for *E. coli* (Sigma)]. The exponential and stationary phases of growth were defined based on the growth curves obtained. For *E. coli*, exponential growth was considered for time points from 2 to 5 hours and stationary growth from 6 to 9 hours. For *M. smegmatis*, the exponential phase of growth was defined for time points from 6 to 12 hours and stationary for time points 24 to 48 hours. Finally, for *M. tuberculosis*, exponential growth phase was considered for time points 2 to 7 days and stationary phase from 8 days.

### DNA manipulations

Mycobacterial genomic DNA was prepared using the InstaGene Matrix kit (BioRad) or the PureLink Genomic DNA Kit (Invitrogen), following manufacturers' instructions. All the oligonucleotides used in this study are listed in Table 1 and were synthesized by Sigma-Aldrich or ITD Technologies. DNA sequences were determined by Source BioScience (<https://www.sourcebioscience.com>) using the Sanger method.

### Construction of luminescent reporter plasmids and strains

The plasmids used in this study are described in Table 2. The integrating expression vector pMV306trpT was created by cloning five copies of the transcriptional terminator trp from pEJ414<sup>23</sup> into pMV306<sup>22</sup> using KpnI+XbaI. Cloning of the terminator was confirmed by sequencing. The firefly luciferase (*ffluc*) gene was PCR amplified using primers FFluc\_EcoRI\_F and FFluc\_Sall\_R (Table 1) containing restriction sites as indicated and using pMV306hsp+FFluc<sup>24</sup> as a template. Primers were designed to only amplify the coding region and hence exclude the optimised Shine-Dalgarno sequence. The sequence of the PCR product was confirmed by DNA sequencing. The FFluc gene was cloned into pMV306trpT after digestion with EcoRI-Sall to create pTC1. The desA1 (Rv0824c) and desA2 (Rv1094) gene pair from *M. tuberculosis* were selected as Shine-Dalgarno and leaderless candidates, respectively. Reporter constructs were generated by fusing the candidate regions from desA1 and desA2 genes to the *ffluc* gene in pTC1 using NcoI-EcoRI as follows: a) the Shine-Dalgarno reporter vector pTC2 was created by fusing the 50 bp promoter region, followed by the 5'UTR and six N-terminal amino acids from desA1; b) the leaderless reporter pTC3 was created by fusing the 50 nt promoter region followed by the six N-terminal amino acids from desA2; c) the Shine-Dalgarno reporter pTC4 was created by swapping the desA1 promoter in pTC2 by the desA2 promoter; and d) the leaderless pTC5 reporter was created by swapping the desA2 promoter in pTC3 by the desA1 promoter. All candidate regions were cloned into pTC1 as oligo cloning and the sequences of the dna oligos are available in Table 1. Briefly, oligos were reannealed by mixing equal volumes of both complementary oligos and placing them in a thermocycler with the following settings: first heat at 95°C for 2 min; second cool down to 25°C and incubate for 45 min and finally cool down to 4°C for further storage. All the sequences from the reporter constructs were confirmed by sequencing. Reporter plasmids were transformed into *E. coli*, and electroporated into *M. smegmatis* and *M. tuberculosis* as previously described<sup>42</sup>. Correct construction of the reporter strains was verified by sequencing of specific PCR amplified regions (Table 1) from either plasmid DNA isolated from *E. coli* or chromosomal DNA isolated from *M. smegmatis* and *M. tuberculosis*. The generated strains were named according to the reporter fusion they carried.

### RNA isolation and determination of transcription start sites (TSSs)

Samples from *M. tuberculosis* pTC2-5 reporter strains were harvested from mid-exponential and stationary phase cultures and immediately processed for RNA extraction. For each sample, 30 mL of culture were spun down and RNA isolated using the FastRNA Pro blue kit (MP Biomedicals) following manufacturer's instructions. All RNA samples were treated with Turbo DNase (Ambion) to remove any DNA contamination. The concentration and quality of RNA samples were assessed by Nanodrop (ND-1000, Labtech) and by running an Agilent RNA chip (2100 Bioanalyser). One microgram of purified RNA was then reverse transcribed into cDNA using the 5'RACE kit from Invitrogen, according to manufacturer's instructions, and the obtained cDNA was further amplified using the specific oligo FFluc\_R1 (Table 1) together with the oligos provided in the 5' RACE kit. Amplified products were sequenced and the TSSs for each construct identified.

### Luciferase activity assays

To assess the translation kinetics of the leaderless and SD reporters, luciferase activity assays were performed. The substrate for FFluc, D-luciferin (Gold Bio?), was prepared in distilled water at 94 mM (30 mg ml<sup>-1</sup>) and filter sterilised. All stocks were stored at -20°C and diluted in equivalent broth media or PBS (without calcium or magnesium) immediately before use. Working solutions were kept on ice in the dark during preparation. For the experiments, two or three independent cultures of each strain were grown as indicated previously, and each culture was measured in duplicate or triplicate at 37°C with a FLUOstar Omega microplate reader (BMG Labtech). For performing the measurements, 96-well polystyrene microplates were prepared with 100 µl sample/well, and 10 µl of D-luciferin solution (final concentration of 150 µg ml<sup>-1</sup>) was injected row by row and luminescence was immediately measured after adding the substrate for 3 s. Equivalent blank samples only containing broth medium were processed in parallel to each experiment and the luminescence measurements treated as the background luminescence. These control values were equivalent to luminescence measurements obtained for adequately processed cultures of *M. tuberculosis*, *M. smegmatis* and *E. coli* carrying the corresponding empty vector pTC1. Data was analysed using the Mars software package (BMG Labtech) to calculate relative light units (RLUs).

### Nutrient starvation experiments

For the nutrient starvation experiments, *M. tuberculosis* H37Rv was grown in 100 ml cultures until mid-exponential phase using 1 L roller bottles (Nalgene). When the cultures reached an OD<sub>600</sub> of 0.4-0.6, cells were harvested, washed twice with PBS and resuspended in 100 ml of fresh PBS supplemented with 0.025% tyloxapol (Sigma). Cultures were then incubated in 1L roller bottles for 28 days. Parallel cultures were kept in 7H9 media as controls. For each reporter tested, two independent transformants were grown. The samples were collected from nutrient-starved and control cultures after 6 hrs, 24 hrs, 48 hrs, 72 hrs, 96 hrs and 120 hrs for luminescence assays and for RNA extraction. Experiments were performed in duplicate.

### Nitric oxide experiments

For the nitric oxide experiments, *M. tuberculosis* H37Rv was grown in 100 ml cultures until mid-exponential phase using 1L roller bottles. Diethylenetriamine/nitric oxide adduct (DETA/NO; Sigma) was prepared by dissolving in 0.1 M NaOH to reach a working concentration of 100 mM. When the cultures reached an OD<sub>600</sub> of 0.4-0.6, DETA/NO was added to a final concentration of 0.25 mM. Cultures were subsequently incubated in 1L roller bottles for 7 days in parallel to control cultures kept in 7H9 with an equivalent concentration of NaOH to that of the DETA/NO cultures. For each reporter tested, two independent transformants were included. Samples were collected after 6 hrs, 24 hrs, 48 hrs, 72 hrs, 96 hrs and 120 hrs for luminescence assays and for RNA extraction. Experiments were performed in duplicate.

### THP-1 cell line culture and macrophage infection experiments

THP-1 line monocytes (ATCC<sup>®</sup>) were cultured routinely in RPMI-1640 medium containing HEPES and L-Glutamine (ThermoFisher Scientific UK Ltd), supplemented into RPMI complete medium with 10% heat-inactivated foetal bovine serum (FBS; Sigma) and 0.05 mM 2-mercaptoethanol (Sigma) at 37°C in 5% CO<sub>2</sub>. The monocytes were differentiated into THP-1 macrophages by using the inducing reagent phorbol 12-myristate 13-acetate (PMA; Sigma) at a final concentration of 0.050 µg ml<sup>-1</sup>. Cells were seeded in 24-well plates at a density of 10<sup>4</sup> cells/well in 500 µL of medium and differentiated for 4 days prior to infection with *M. tuberculosis*. Mid-log phase cultures of *M. tuberculosis* reporter strains were washed twice with PBS, diluted in RPMI-1640 and added to THP-1 macrophage layers at a concentration of 10<sup>5</sup> CFU/well (MOI of 10). After 3 hrs of infection at 37°C in 5% CO<sub>2</sub>, macrophages were washed twice with Hank's Balanced Salt Solution (HBSS) (ThermoFisher Scientific UK Ltd) to eliminate any extracellular bacteria. Lastly, 0.5 ml of complete RPMI was added to each well. Cells were either immediately processed or incubated further to reach 24 hrs, 48 hrs, 72 hrs, 96 hrs, and 168 hrs (7 days) post-infection. Bacterial intracellular survival and growth were assessed by lysis of the monolayers after addition of 0.1% Triton X-100 in HBSS and enumeration of bacteria by plating of serial dilutions in PBS-Tween onto 7H11 medium. Colonies were counted after 3-4 weeks and their count confirmed after 6 weeks of incubation at 37°C and the average CFU/ml determined. Infection experiments were conducted in triplicate.

### RNA isolation and q-RT PCR

For the quantification of transcript levels through quantitative real-time PCR, parallel samples to the ones used for the luminescence screens were harvested for RNA isolation. For each sample, 10 mL of culture were spun down and RNA isolated using the FastRNA Pro blue kit (MP Biomedicals), following manufacturer's instructions. All RNA samples were treated with Turbo DNase (Ambion) to remove any DNA contamination. The concentration and quality of the RNA samples were assessed by Nanodrop (ND-1000, Labtech) and by running an Agilent RNA chip (2100 Bioanalyser). Either 500 ng or 1 µg of the purified RNA were used for reverse transcription into cDNA using the High-Capacity cDNA Reverse Transcription kit (Applied Biosystems). Quantitative real-time PCR was carried out on a 7500 Fast Real-Time PCR system (Applied Biosystems) and using the KAPA SYBR FAST kit (Applied Biosystems), following the manufacturer's protocol. Specific primers targeting the 16s rRNA were used as an (Table 1) internal control. Relative quantification of the expression levels was calculated using the 2<sup>- $\Delta\Delta$ CT</sup> method<sup>43</sup>.

### Statistical analysis

Statistical analysis was performed using GraphPad Prism 9.0.1 (GraphPad Software, San Diego, California USA, www.graphpad.com). Data was tested for normal distribution using the D'Agostino & Pearson omnibus test. Differences in translation efficiencies between reporters were assessed using unpaired multiple t tests with False Discovery Rate correction when comparing two groups, or by one-way ANOVA with Dunn's correction for multiple testing when comparing more than two groups. Non-parametric analysis was performed using the Mann-Whitney test or the Kruskal-Wallis test when comparing two or more groups respectively.

## Declarations

### Acknowledgments

This work was supported by funding from the European Research Council (ERC) under the European Union's Horizon 2020 research and innovation programme (grant agreement No 637730).

### Author Contributions

NA created the pMV306trpT integrating vector and with TC and ADG designed the translational reporters. ADG and TC conceived and designed the experiments. ADG performed the experiments. ADG and TC analysed the data. ADG and TC wrote the paper. NA reviewed the paper. All authors read and approved the final manuscript

### Additional Information

The authors declare no competing financial and non-financial interests in relation to the work here described.

## References

1. Global tuberculosis report 2019. (2019).

2. Houben, R. M. G. J. & Dodd, P. J. The Global Burden of Latent Tuberculosis Infection: A Re-estimation Using Mathematical Modelling. *PLOS Med.* **13**, e1002152 (2016).
3. Forrellad, M. A. et al. Virulence factors of the *Mycobacterium tuberculosis complex*. *Virulence* **4**, 3–66 (2013).
4. Ehrh, S., Schnappinger, D. & Rhee, K. Y. Metabolic principles of persistence and pathogenicity in *Mycobacterium tuberculosis*. *Nature Reviews Microbiology* (2018) doi:10.1038/s41579-018-0013-4.
5. Bentrup, K. H. zu & Russell, D. G. Mycobacterial persistence: Adaptation to a changing environment. *Trends in Microbiology* (2001) doi:10.1016/S0966-842X(01)02238-7.
6. Xue, S. & Barna, M. Specialized ribosomes: a new frontier in gene regulation and organismal biology. *Nat. Rev. Mol. Cell Biol.* **13**, 355–369 (2012).
7. Byrgazov, K., Vesper, O. & Moll, I. Ribosome heterogeneity: Another level of complexity in bacterial translation regulation. *Current Opinion in Microbiology* vol. 16 133–139 (2013).
8. Shine, J. & Dalgarno, L. The 3' terminal sequence of *Escherichia coli* 16S ribosomal RNA: complementarity to nonsense triplets and ribosome binding sites. *Proc. Natl. Acad. Sci. U. S. A.* **71**, 1342–1346 (1974).
9. Zheng, X., Hu, G.-Q., She, Z.-S. & Zhu, H. Leaderless genes in bacteria: clue to the evolution of translation initiation mechanisms in prokaryotes. *BMC Genomics* **12**, 361 (2011).
10. Nakagawa, S., Niimura, Y. & Gojobori, T. Comparative genomic analysis of translation initiation mechanisms for genes lacking the Shine–Dalgarno sequence in prokaryotes. *Nucleic Acids Res.* **1121**, 1–10 (2017).
11. Beck, H. J., Fleming, I. M. C. & Janssen, G. R. 5'-Terminal AUGs in *Escherichia coli* mRNAs with Shine-Dalgarno sequences: Identification and analysis of their roles in non-canonical translation initiation. *PLoS One* **11**, (2016).
12. Udagawa, T., Shimizu, Y. & Ueda, T. Evidence for the translation initiation of leaderless mRNAs by the intact 70 S ribosome without its dissociation into subunits in eubacteria. *J. Biol. Chem.* **279**, 8539–46 (2004).
13. Vesper, O. et al. Selective translation of leaderless mRNAs by specialized ribosomes generated by MazF in *Escherichia coli*. *Cell* **147**, 147–157 (2011).
14. Kaberdina, A. C., Szaflarski, W., Nierhaus, K. H. & Moll, I. An Unexpected Type of Ribosomes Induced by Kasugamycin: A Look into Ancestral Times of Protein Synthesis? *Mol. Cell* **33**, 227–236 (2009).
15. Cortes, T. et al. Genome-wide Mapping of Transcriptional Start Sites Defines an Extensive Leaderless Transcriptome in *Mycobacterium tuberculosis*. *Cell Rep.* **5**, 1121–1131 (2013).
16. Shell, S. S. et al. Leaderless Transcripts and Small Proteins Are Common Features of the Mycobacterial Translational Landscape. *PLoS Genet.* **11**, (2015).
17. Kröger, C. et al. The transcriptional landscape and small RNAs of *Salmonella enterica* serovar Typhimurium. *Proc. Natl. Acad. Sci. U. S. A.* **109**, E1277-86 (2012).
18. Seo, J. H. et al. Multiple-omic data analysis of *Klebsiella pneumoniae* MGH 78578 reveals its transcriptional architecture and regulatory features. *BMC Genomics* **13**, 679 (2012).
19. Sharma, C. M. et al. The primary transcriptome of the major human pathogen *Helicobacter pylori*. *Nature* **464**, 250–255 (2010).
20. Thomason, M. K. et al. Global transcriptional start site mapping using differential RNA sequencing reveals novel antisense RNAs in *Escherichia coli*. *J. Bacteriol.* (2015) doi:10.1128/JB.02096-14.
21. Nguyen, T. G., Vargas-Blanco, D. A., Roberts, L. A. & Shell, S. S. The impact of leadered and leaderless gene structures on translation efficiency, transcript stability, and predicted transcription rates in *Mycobacterium smegmatis*. *J. Bacteriol.* (2020) doi:10.1128/JB.00746-19.
22. Stover, C. K. et al. New use of BCG for recombinant vaccines. *Nature* (1991) doi:10.1038/351456a0.
23. Papavinasandaram, K. G. et al. Slow induction of RecA by DNA damage in *Mycobacterium tuberculosis*. *Microbiology* (2001) doi:10.1099/00221287-147-12-3271.
24. Andreu, N. et al. Optimisation of bioluminescent reporters for use with mycobacteria. *PLoS One* **5**, e10777 (2010).
25. Moll, I., Grill, S., Gualerzi, C. O. & Bläsi, U. Leaderless mRNAs in bacteria: Surprises in ribosomal recruitment and translational control. *Mol. Microbiol.* **43**, 239–246 (2002).
26. Betts, J. C., Lukey, P. T., Robb, L. C., McAdam, R. A. & Duncan, K. Evaluation of a nutrient starvation model of *Mycobacterium tuberculosis* persistence by gene and protein expression profiling. *Mol. Microbiol.* **43**, 717–731 (2002).
27. Robinson, J. L., Adolfsen, K. J. & Brynildsen, M. P. Deciphering nitric oxide stress in bacteria with quantitative modeling. *Curr. Opin. Microbiol.* **19**, 16–24 (2014).
28. Nathan, C. Role of iNOS in human host defense. *Science (New York, N.Y.)* vol. 312 1874–1875 (2006).
29. Sawyer, E. B., Phelan, J. E., Clark, T. G. & Cortes, A snapshot of translation in *Mycobacterium tuberculosis* during exponential growth and nutrient starvation revealed by ribosome profiling. *Cell Reports* **34(5)**, 108695 (2021).
30. Moll, I., Hirokawa, G., Kiel, M. C., Kaji, A. & Bläsi, U. Translation initiation with 70S ribosomes: An alternative pathway for leaderless mRNAs. *Nucleic Acids Res.* **32**, 3354–3363 (2004).

31. Moll, I. & Engelberg-Kulka, H. Selective translation during stress in *Escherichia coli*. Trends Biochem. Sci. **37**, 493–498 (2012).
32. Yang, K. et al. Structural insights into species-specific features of the ribosome from the human pathogen *Mycobacterium tuberculosis*. Nucleic Acids Res. (2017).
33. Hentschel, J. et al. The Complete Structure of the *Mycobacterium smegmatis* 70S Ribosome. Cell Rep. **20**, 149–160 (2017).
34. Chen, Y.-X. et al. Selective translation by alternative bacterial ribosomes. Proc. Natl. Acad. Sci. **117**, 19487 LP – 19496 (2020).
35. Dow, A. & Priscic, S. Alternative ribosomal proteins are required for growth and morphogenesis of *Mycobacterium smegmatis* under zinc limiting conditions. PLoS One **13**, e0196300 (2018).
36. Priscic, S. et al. Zinc regulates a switch between primary and alternative S18 ribosomal proteins in *Mycobacterium tuberculosis*. Mol. Microbiol. **97**, 263–280 (2015).
37. Li, X. et al. Structure of ribosomal silencing factor bound to *Mycobacterium tuberculosis* ribosome. Structure **23**, 1858–1865 (2015).
38. Trauner, A., Loughheed, K. E. A., Bennett, M. H., Hingley-Wilson, S. M. & Williams, H. D. The dormancy regulator DosR controls ribosome stability in hypoxic mycobacteria. J. Biol. Chem. **287**, 24053–24063 (2012).
39. Sachdeva, P., Misra, R., Tyagi, A. K. & Singh, Y. The sigma factors of *Mycobacterium tuberculosis*: Regulation of the regulators. FEBS Journal (2010) doi:10.1111/j.1742-4658.2009.07479.x.
40. Newton-Foot, M. & Gey Van Pittius, N. C. The complex architecture of mycobacterial promoters. Tuberculosis vol. 93 60–74 (2013).
41. Snapper, S. B., Melton, R. E., Mustafa, S., Kieser, T. & Jr, W. R. J. Isolation and characterization of efficient plasmid transformation mutants of *Mycobacterium smegmatis*. Mol. Microbiol. **4**, 1911–1919 (1990).
42. Goude, R., Roberts, D. M. & Parish, T. Electroporation of mycobacteria. Methods Mol. Biol. (2015) doi:10.1007/978-1-4939-2450-9\_7.
43. Livak, K. J. & Schmittgen, T. D. Analysis of relative gene expression data using real-time quantitative PCR and the 2- $\Delta\Delta$ CT method. Methods **25**, 402–408 (2001).

## Tables

Table 1. Primers used in this study

Primer name	Primer sequence <sup>a</sup>	Target
FFluc-EcoRI-F	5'- <i>ccgaggaattc</i> atggaagatgcaagaacatca-3'	FFluc
FFluc-SalI-R	5'- <i>aggctgctgact</i> ctagagtcacttgccct-3'	
pMV-Up	5'-aacctgattaccgctttga-3'	pMV306tpdT,
pMV-Down	5'-tccttcgactgaccccttcg-3'	pTC1-5
Oligo-pTC2-top	5'- <b>CATGG</b> gcgcgaagcccaactgatgctaccgagagacacagatataatgactgcaaccattagacacagataactggaggcgccatgtcagccaagctgacc <b>G-3'</b>	<i>desA1</i> candidate region
Oligo-pTC2-bottom	5'- <b>AATTC</b> ggctcagctggctgacatggcgctccagttactgtgtctaatggtgagctcaatatactgtgtctctcggtagcatcaagttgggcttcgccc <b>C-3'</b>	
Oligo-pTC3-top	5'- <b>CATGG</b> cgccggcgcccgatcttcacgaaatctgtgtatgaggttacagttaccgc <b>atggc</b> acagaa <b>acctgtcG-3'</b>	<i>desA2</i> candidate region
Oligo-pTC3-bottom	5'- <b>AATTC</b> gacaggtttctgtgccatgctgtaactgtaactgcatacacagattctgtgaaatcgggcgccgccc <b>C-3'</b>	
Oligo-pTC4-top	5'- <b>CATGG</b> cgccggcgcccgatcttcacgaaatctgtgtatgaggttacagttaccgcaaccattagacacagataactggaggcgccatgtcagccaagctgacc <b>G-3'</b>	<i>desA1</i> candidate region with <i>desA2</i> promoter swapped
Oligo-pTC4-bottom	5'- <b>AATTC</b> ggctcagctggctgacatggcgctccagttactgtgtctaatggtggcggttaactgtaactgcatacacagattctgtgaaatcgggcgccgccc <b>C-3'</b>	
Oligo-pTC5-top	5'- <b>CATGG</b> gcgcgaagcccaactgatgctaccgagagacacagatataatgactg <b>atggc</b> acagaa <b>acctgtcG-3'</b>	<i>desA2</i> candidate region with <i>desA1</i> promoter swapped
Oligo-pTC5-bottom	5'- <b>AATTC</b> gacaggtttctgtgccatcagtcaatatactgtgtctctcggtagcatcaagttgggcttcgccc <b>C-3'</b>	
FFluc-PCR1-F	5'-cgttctaccgctggaggac-3'	pTC1-5
FFluc-PCR1-R	5'-tcttgaggctacgcaagaaca-3'	pTC1-5
FFluc-PCR2-F	5'-gcccctgttggtccc-3'	pTC1-5
FFluc-PCR2-R	5'-cgatcgtagctgtaactacgctcg-3'	pTC1-5
pMV_FFluc_R1	5'-gatgtgcatcggtgaagg-3'	pTC1-5
GSP1	5'-tggaaccgcttcgcaaggc-3'	pTC2-5
GSP2A	5'-cgacgcatctcgtgagattcg-3'	pTC2-5
GSP2B	5'-gcccgaagtggagctgagc-3'	pTC2-5
16s-F	5'-aagaagcaccggccaactac-3'	16s rRNA
16s-R	5'-tcgctcctcaggtcagta-3'	16s rRNA

<sup>a</sup>In italics, sequence added to include restriction sites (underlined) for cloning procedures. For the DNA oligos, in capitals red, bases added to complement the overhangs generated during cloning procedures; in highlighted yellow, -10 promoter motif; in bold, transcription start site as described in Cortes et al<sup>15</sup> highlighted grey, 5'UTR sequence; in highlighted green, SD sequence; underlined, sequence corresponding to the six N-terminal amino acids with the start codon highlighted in red.

Table 2. Vectors used in this study

Vector	Description	Reference or source
pEJ414	pMV306 derivative containing a promoterless <i>E. coli lacZ</i> gene	[23]
pMV306	Mycobacterial integrating vector, Km <sup>r</sup>	[22]
pMV306hsp+FFluc	pMV306 derivative containing $P_{hsp60}$ and the firefly luciferase (FFluc) codon optimized for <i>M. tuberculosis</i>	[24]
pMV306trpT	pMV306 derivative containing 5 copies of transcriptional terminator from pEJ414	This study
pTC1	pMV306trpT derivative encoding the firefly luciferase gene (FFluc) excluding the SD sequence	This study
pTC2	pTC1 derivative containing $P_{desA1}$ :UTR <sub>desA1</sub> :6 N-terminal aa <sub>desA1</sub>	This study
pTC3	pTC1 derivative containing $P_{desA2}$ :6 N-terminal aa <sub>desA2</sub>	This study
pTC4	pTC1 derivative containing $P_{desA2}$ :UTR <sub>desA1</sub> :6 N-terminal aa <sub>desA1</sub>	This study
pTC5	pTC1 derivative containing $P_{desA1}$ :6 N-terminal aa <sub>desA2</sub>	This study

## Figures

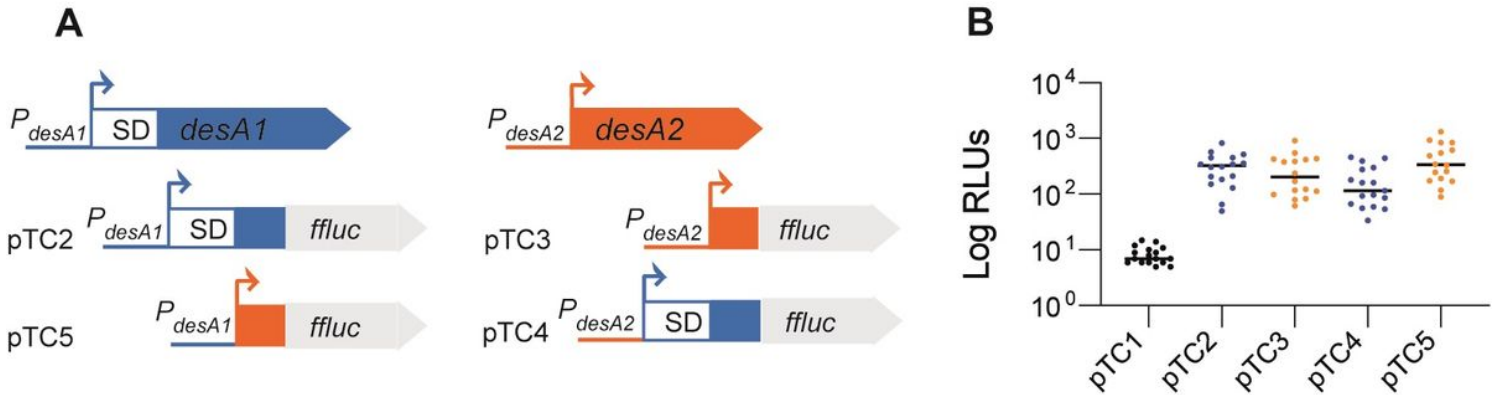


**Figure 1**

Construction of leaderless and Shine-Dalgarno luminescent reporter strains in *M. tuberculosis*. (A) Schematic representation of the translational reporters constructed using the *M. tuberculosis desA1* and *desA2* genes. All reporters were constructed using the pTC1 vector as backbone. Promoter regions of *desA1* and *desA2* are represented as blue and orange lines, respectively, and the sequence encoding the first 6 amino acids of *desA1* and *desA2* are represented as blue and orange boxes, respectively. For *desA1*, the 5'UTR including the Shine-Dalgarno (SD) sequence is represented as a white box with blue borders. (B) Bioluminescence in *M. tuberculosis* transformed with the reporter vectors. For each reporter, luminescence of two independent *M. tuberculosis* transformants was measured daily over 5 days of exponential growth. Results are given as relative light units (RLUs) and are corrected by the optical density. Each dot represents one measurement and bars indicate median values.

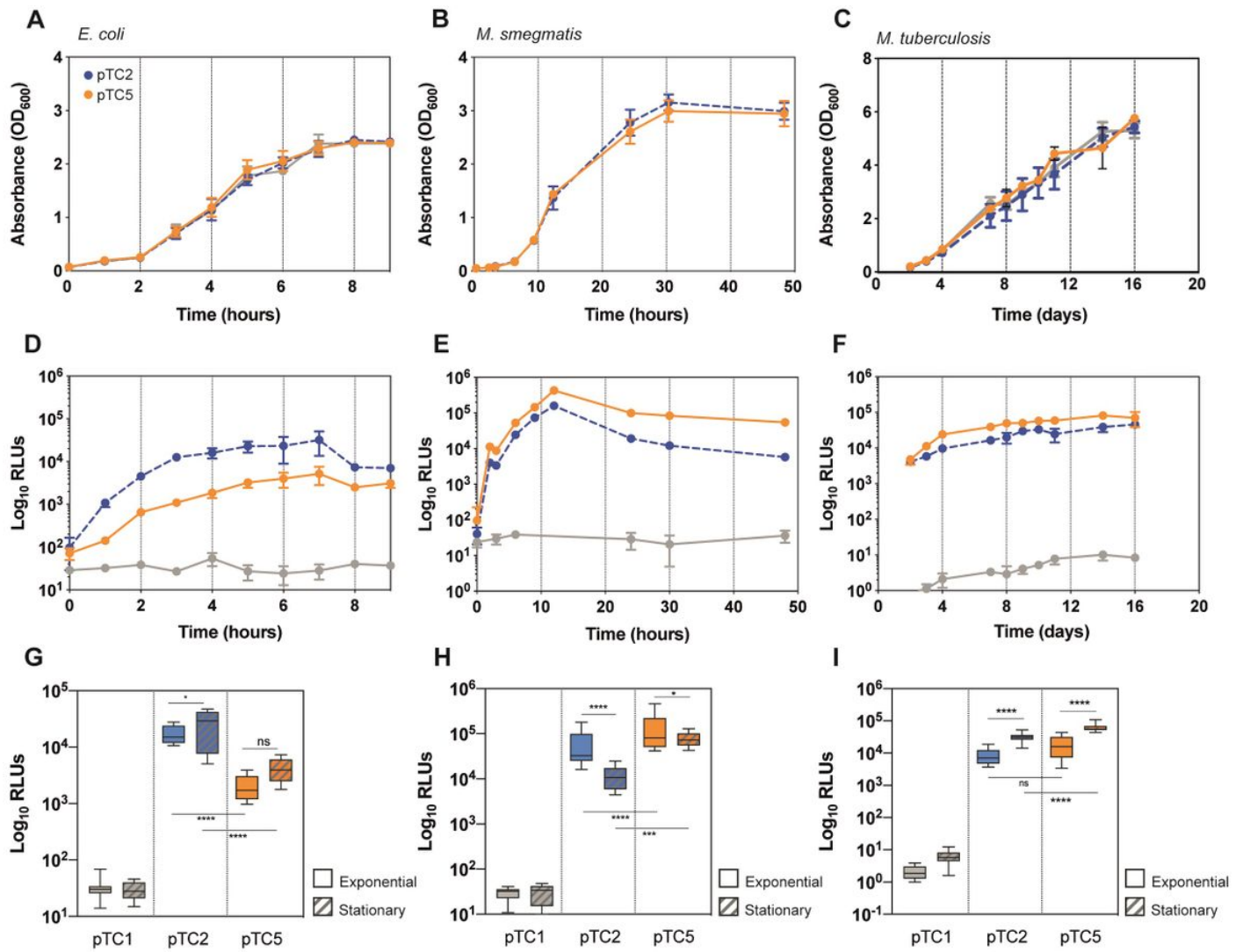


**Figure 2**

Growth and translation kinetics of leaderless and Shine-Dalgarno reporters in three bacterial models during in vitro growth. Bacterial growth curves of *E. coli* (A), *M. smegmatis* (B) and *M. tuberculosis* (C) and luminescence measured in *E. coli* (D), *M. smegmatis* (E) and *M. tuberculosis* (F) transformed with pTC1 (grey), pTC2 (Shine-Dalgarno, blue) and pTC5 (leaderless, orange). The vectors are replicative in *E. coli* and integrative in mycobacteria. Cultures were inoculated to an initial OD ~ 0.1 and growth (expressed as OD<sub>600</sub>) and luminescence (expressed as relative light units, RLUs) were measured over 9 hours for *E. coli* (A and D), 48 hours for *M. smegmatis* (B and E) and 16 days for *M. tuberculosis* (C and F). For each timepoint and reporter at least three independent transformants were analyzed and each experiment was performed in triplicate. The mean value and standard deviation are presented. Luminescence levels during exponential growth (clear boxes) and stationary phase (patterned boxes) in *E. coli* (G), *M. smegmatis* (H) and *M. tuberculosis* (I) transformed with the indicated vectors. Box plots indicate median (horizontal line), interquartile range (box) and maximum and minimum values (whiskers). Medians were compared using one-way ANOVA. \*p < 0.05, \*\*\*p < 0.001, \*\*\*\*p < 0.0001, ns: non-significant.

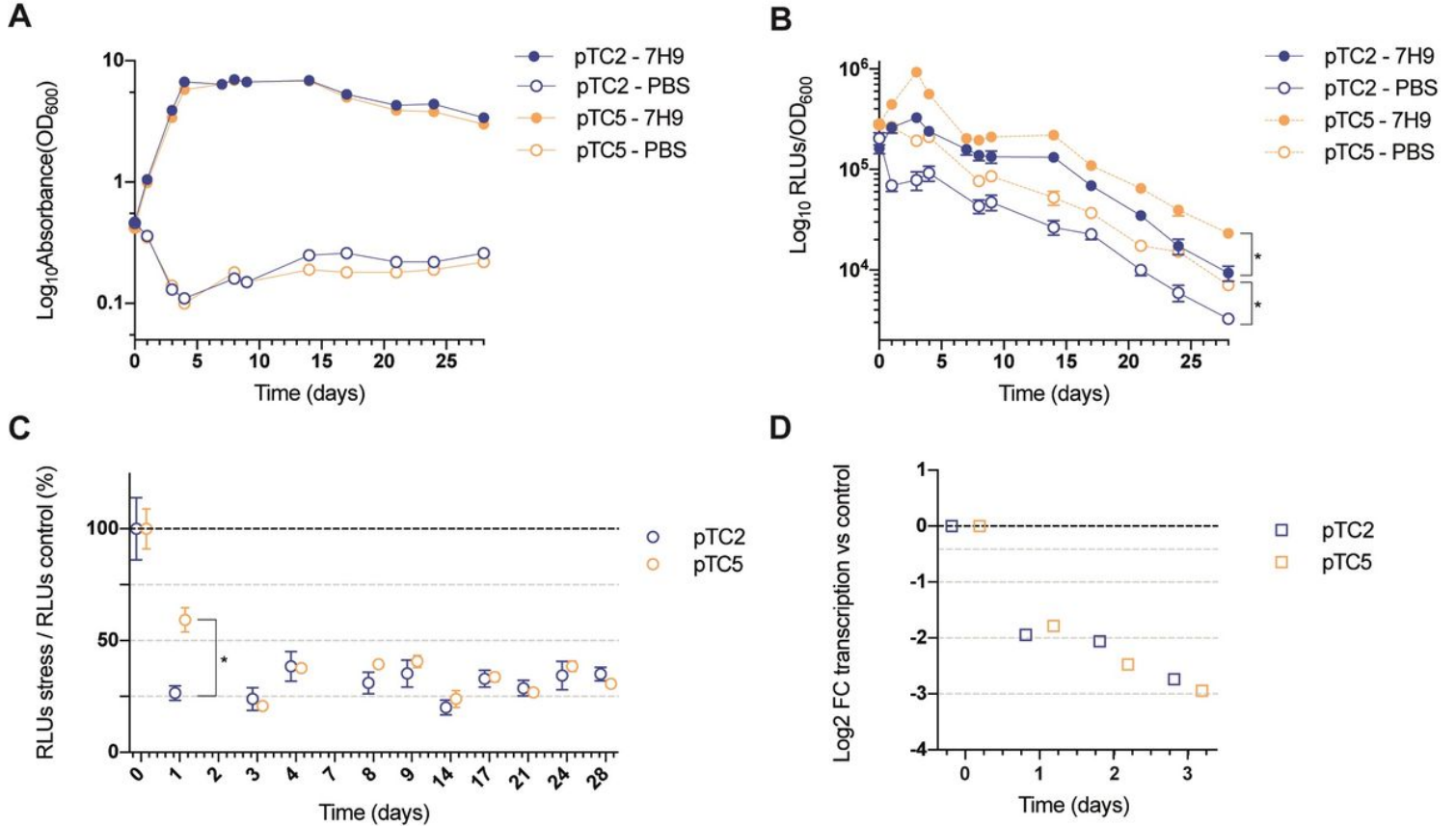


**Figure 3**

Growth and translation kinetics of the leaderless and Shine-Dalgarno reporters during nutrient starvation. Cultures of *M. tuberculosis* carrying integrative vectors pTC2 (Shine-Dalgarno (SD), blue) and pTC5 (leaderless (L), orange) were grown to mid-exponential phase (time 0), washed and resuspended in PBS (PBS) or kept in rich media as controls (7H9). For each timepoint and reporter at least three independent transformants were used and measurements were done in triplicate; the mean value and standard deviation are presented. (A) OD<sub>600</sub> was monitored for 28 days. (B) Luminescence, given as relative light units (RLUs) corrected by growth. Asterisks denote statistically significant differences between pTC2 and pTC5 reporters for all timepoints in each condition (multiple t-tests,  $p < 0.001$ ). (C) To calculate the overall effect that nutrient starvation has on the translation of the reporters, for each timepoint and reporter, the RLU value during nutrient starvation was normalised against the RLU control value. The value obtained at time 0 was considered as the 100% translation efficiency. Statistically significant differences are indicated with an asterisk (multiple t-tests,  $p < 0.001$ ). (D) Quantification of transcription levels by real-time PCR. Fold changes (FC) are relative to transcript levels in control cultures (7H9) and expressed as log<sub>2</sub>.

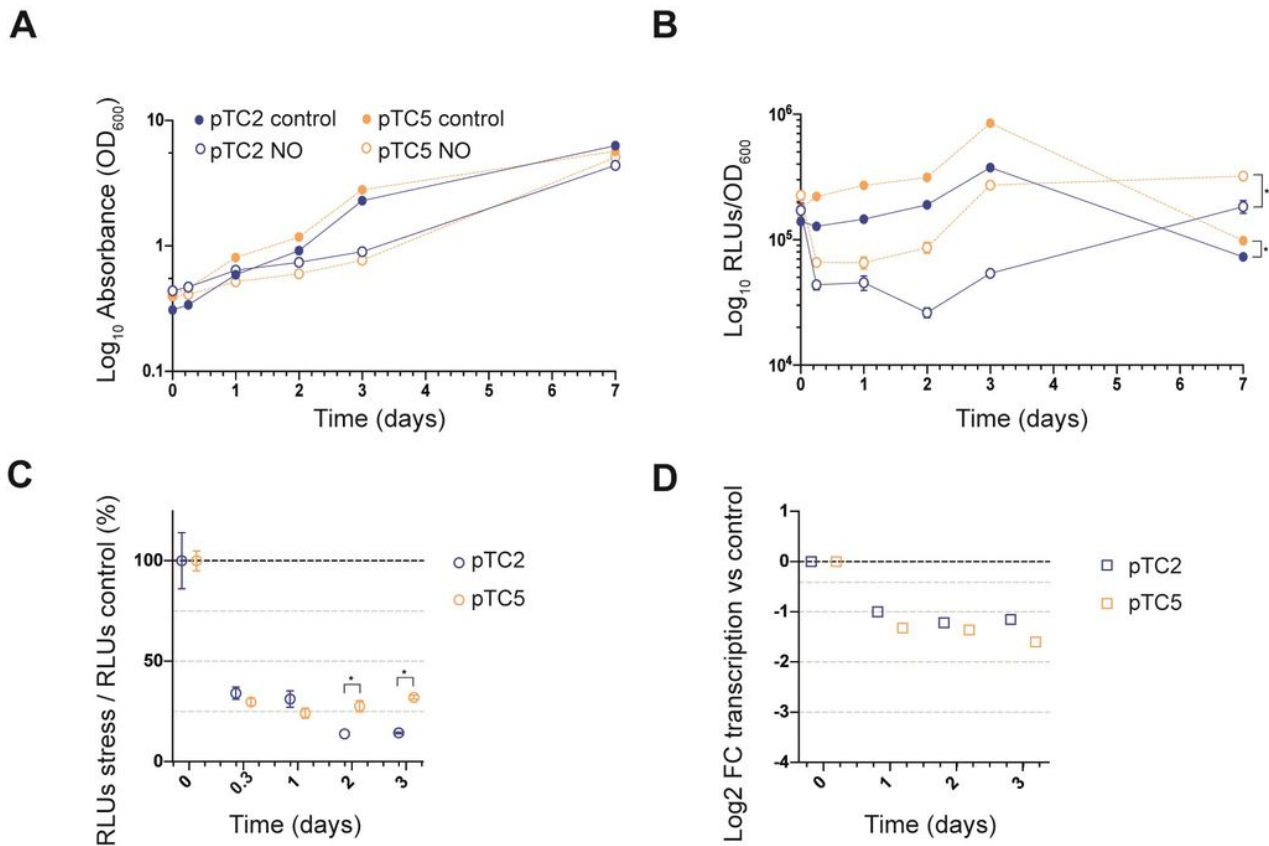


**Figure 4**

Growth and translation kinetics of the leaderless and Shine-Dalgarno reporters during nitric oxide (NO) stress. Cultures of *M. tuberculosis* carrying integrative vectors pTC2 (Shine-Dalgarno (SD), blue) and pTC5 (leaderless (L), orange) were grown to mid-exponential phase (time 0) when cells were either challenged with 0.25 mM NO or the vehicle NaOH as control. For each timepoint and reporter at least three independent transformants were used and measurements were done in triplicate; the mean and standard deviation are presented. (A) OD<sub>600</sub> was monitored for 7 days. (B) Luminescence, given as relative light units (RLUs) corrected by growth. Asterisks denote statistically significant differences between pTC2 and pTC5 reporters for all timepoints in each condition (multiple t-tests,  $p < 0.03$ ). (C) The RLU value during NO challenge was normalised against the corresponding RLU control value. The value obtained at time 0 was considered as 100% translation efficiency. Statistically significant differences are indicated with an asterisk (multiple t-tests,  $p < 0.002$ ). (D) Quantification of transcription levels by real-time PCR. Fold changes (FC) are relative to the corresponding control and expressed as log<sub>2</sub>.

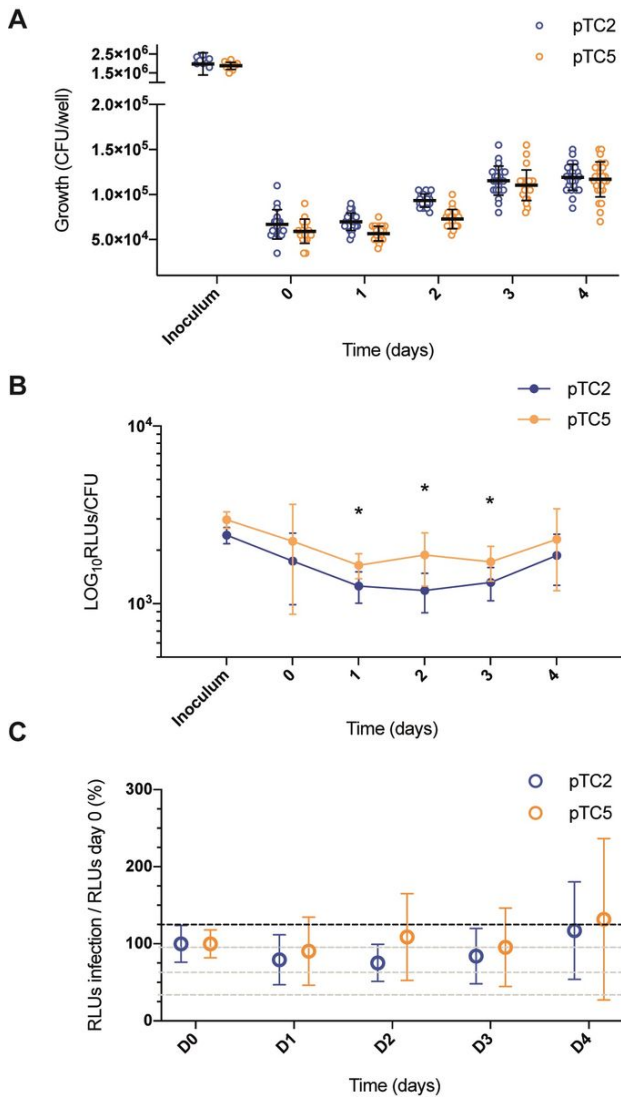


**Figure 5**

Growth and luminescence production of the leaderless and Shine-Dalgarno reporter strains during infection of THP-1 cells. (A) CFU were counted for 4 days post-infection of THP-1 cells with the *M. tuberculosis* leaderless (orange) and Shine-Dalgarno (blue) reporter strains. (B) Luminescence, given as relative light units (RLUs). Statistically significant differences at day 1, day 2 and day 3 post infection are indicated with an asterisk (multiple t-tests,  $p < 0.002$ ). (C) To calculate the overall effect that infection of THP-1 cells has on the translation of the reporters, for each timepoint and reporter, the RLU value during macrophage infection was normalised against the RLU after bacterial internalisation (time 0). The value obtained at time 0 was considered as the 100% translation efficiency. All experiments were performed in triplicate.

## Supplementary Files

This is a list of supplementary files associated with this preprint. Click to download.

- [SF1.pdf](#)